

Electromagnetic Crystal (EMXT) based THz Components

Ziran Wu^a, Wei-Ren Ng^b, Michael Gehm^{b, c}, Hao Xin^{*b, d}

^aStanford Linear Accelerator Center, 2575 Sand Hill Road, Menlo Park, CA USA 94025;

^bElectrical and Computer Engineering Dept., University of Arizona, 1230 E. Speedway Blvd.,

Tucson, AZ USA 85721; ^cCollege of Optical Sciences, University of Arizona, 1630 E. University Blvd., Tucson, AZ USA 85721; ^dPhysics Dept., University of Arizona, 1118 E. 4th Street, Tucson, AZ USA 85721;

ABSTRACT

Various all-dielectric electromagnetic crystal (EMXT) based THz components, including filter/reflector, waveguide, antenna, and transition structure to planar circuits are proposed and simulated. Several of them have been fabricated via a THz rapid prototyping technique, and the measurements show very good consistency with the simulations. Potential integrated THz micro-systems could be constructed using these components. The layer-by-layer printing virtue of the rapid prototyping technique may enable the integration and packaging of various THz components in a systematic manner.

Keywords: Terahertz, electromagnetic crystal, rapid prototyping, integrated system

1. INTRODUCTION

Terahertz (THz) spectrum (100 GHz–10 THz) is a frequency range filled with a plethora of physical, chemical and biological sciences, as well as a great deal of engineering potentials. THz related research is blooming in recent years, driven by interests and applications from broad fields such as astronomic and atmospheric spectroscopy, medical and biological imaging, security screening and remote sensing, and next-generation communications¹. However, one of the obstacles that hurdle the advancement of THz research has been the paucity of THz components, such as guiding structures, filters and reflectors, antennas, and quasi-optics. In addition, efficient and low-cost integration and packaging techniques for THz micro-systems are necessary before wide range of applications can be realized.

This paper reports on various building blocks of potential THz micro-systems, including filter/reflector, waveguide, antenna and transition to planar circuit. Due to the layer-by-layer printing nature of the proposed THz prototyping technique, these components may be integrated and packaged in a systematic manner to realize fully functional THz micro-systems.

2. VARIOUS THz COMPONENTS REALIZED

2.1 THz Rapid Prototyping

We have developed a polymer jetting rapid prototyping technique² for THz wavelength scale fabrication. This fast and inexpensive fabrication method allows 3-D arbitrary shaped structures to be printed using polymer build material. The fabrication process involves decomposing the 3-D geometry of a THz component into a series of layered slices in a CAD program, each representing a 16 μm thick region of the model. As earlier slices provide the surface upon which later slices are constructed, the slice description consists of two different material types—a model material which is assigned to regions that are actually part of the cross-section of the desired object, and a water soluble support material, which is used to provide a base upon which the model sections of future slices can rest, and can be removed after the entire model is complete. The data describing the slices are sent sequentially to the prototyping machine. A series of print heads, much like the print heads of an inkjet printer, deposit a thin layer of UV-curable polymer onto the construction tray. UV lamps on the print head immediately cure materials as they are being deposited, and the final solid structure forms. Metallization of the polymer prototypes and mixing of various printing materials with different properties can be explored to ultimately achieve arbitrary spatial material distributions.

2.2 Three-dimensional THz EMXT Structures

Several 3-D THz EMXT structures have been successfully fabricated by this method. Excellent agreements between simulated and measured THz responses of these structures validate the accuracy and fabrication flexibility of this rapid-prototyping method. Figure 1 shows one example of the well-known woodpile structure (WPS) realized at THz wavelengths.

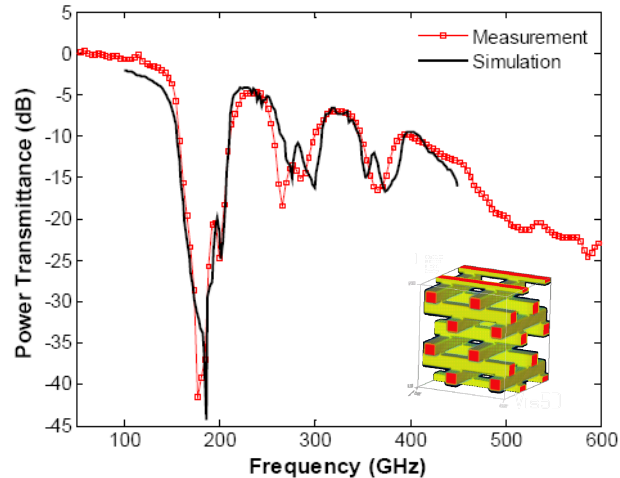


Figure 1. Comparison between the measured (open squares) and simulated (solid line) WPS normal-incidence power transmittances.

As shown in the inset, the WPS has a square rod with a side dimension of $352\ \mu\text{m}$ and a rod spacing of $1292\ \mu\text{m}$ in each stacking layer. In the stacking direction, it consists of 5 unit cells (20 layers of rods). The structure is directly printed using the THz rapid prototyping approach, and its power transmittance is measured via a THz time-domain spectrometer (THz-TDS). In Figure 1, it is seen that the fabricated polymer WPS exhibits a fundamental electromagnetic band gap (EBG) at around 180 GHz, with a band rejection of more than 35 dB. The secondary and tertiary band gaps at 278 GHz and 372 GHz, respectively, are also observed in the measured power transmittance. Using -15 dB as the criteria of band edges, the sample has a main EBG bandwidth of 48 GHz. Its full bandwidth to mid-gap frequency ratio $\Delta f / f_0$ is therefore around 26.7%. The excellent consistency between the measurement and the simulation (done by the finite-element simulation tool HFSS) results confirms the fabrication accuracy of the polymer jetting technique. The measured EBG performance qualifies this polymer WPS as a good band pass / stop filter.

2.3 THz EMXT Waveguide

Many THz applications have employed free-space propagation, resulting in weak beam confinement, vulnerability to environment fluctuations, and relatively large systems. THz waveguides on the other hand provide a promising approach to overcome these drawbacks, and may lead to compact and low-cost integrated systems. Various types of THz waveguide have been proposed and studied, including metallic rectangular/circular, parallel-plate, plastic fiber, photonic crystal fiber, metal wire, coaxial, etc.⁵. However, realization of a THz waveguide with low transmission loss is still a challenge in all aspects, including performance, fabrication and component integration.

Our group has demonstrated an all-dielectric THz waveguide based on a hollow-core EMXT fiber design³. The waveguide is based on a triangular-lattice air-cylinder array in a dielectric background. Because of the Bragg diffraction in the lattice, this structure exhibits electromagnetic band gaps (EBGs) in certain frequency bands. Within the EBGs, wave propagation is prohibited in the lattice, therefore the structure is able to confine the wave propagation. If a defect is present, this structure will support wave propagation along the defect channel in the band gap frequency, whereas the radiation loss along the propagation path will be greatly suppressed because of the EBG cladding. More importantly, the wave suffers much less material loss than in a conventional optical fiber, because majority of the power is confined within the hollow defect⁴. Therefore, this waveguide structure is quite promising to achieve low transmission loss.

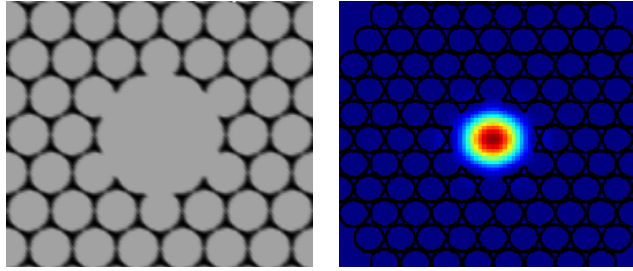


Figure 2. Left: Schematic of the waveguide structure cross section. Right: Energy distribution of HE_{11} mode in the waveguide.

Figure 2, left shows the cross-sectional schematic of the waveguide structure. It has a large air-hole defect at the center. Cladding rings of air cylinders form a triangular lattice and surround the defect. The image on the right shows the energy distribution of the fundamental HE_{11} mode within the first band gap. Simulation reveals that approximately 91% of the power is concentrated within the central defect for this propagating mode. This waveguide schematic is completely scalable. In our design, a lattice constant of 3 mm is applied, which results in center defect radius of 4.2 mm and cladding air cylinder radius of 1.3 mm. Dielectric wall thickness at its thinnest place is 400 μm in this case. The simulated operating frequency of the fundamental HE_{11} mode is around 112 GHz.

The waveguide fabrication has been implemented using the THz rapid prototyping technique. Five waveguides of lengths 50, 75, 100, 125, and 150 mm and identical cross section are fabricated to enable THz-TDS characterization of its propagation loss factor. They are illuminated by an incident linear-polarized THz Gaussian beam, and their transmitted waveforms measured. Fourier transformation of the measured waveforms yields the transmitted power spectra. Figure 3 depicts the measured power transmittance spectra of these five EMXT waveguides.

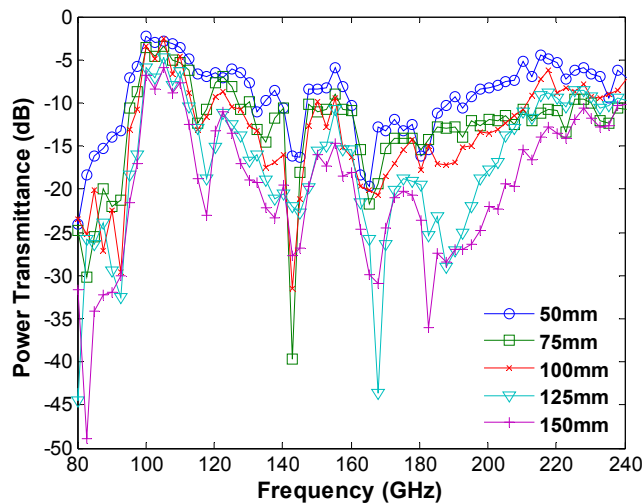


Figure 3. Normalized power transmissions of five waveguides with different lengths and identical cross-section.

Since the coupling between the incident wave and the waveguide at the input end is kept the same, the transmitted (single trip) power follows an exponential decay as the waveguide length increases. Extraction of the waveguide loss factor can therefore be done through a linear fitting process using the transmitted power in dB vs. waveguide length semi-log plot at each frequency. Inset of Figure 4 below shows an example of the extraction process at 107 GHz. The transmitted power (dB) at 107 GHz indeed follows a linear decrease as the waveguide length increases. The absolute value of the slope is the waveguide power loss factor. As shown in Figure 4, the extracted power loss factor spectrum agrees pretty well with our simulation results, except a downshift of about 7 GHz which may be caused by fabrication uncertainties. The lowest waveguide power loss demonstrated is 0.03 dB/mm at 105.2 GHz.

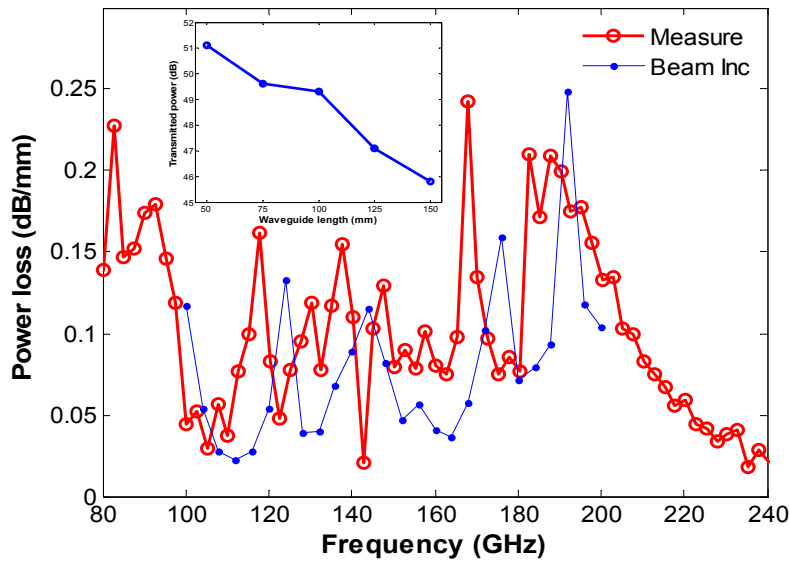


Figure 4. Measured and simulated waveguide power loss with incident Gaussian beam excitation. Inset shows the semi-log fitting process to extract the power loss factor at 107 GHz.

2.4 THz EMXT Horn Antenna

Based on this waveguide design, an EMXT horn antenna is designed by flaring out the waveguide channel radius from 4.2 mm to 8 mm. The antenna is simulated with a circular waveguide (TE_{11} mode) made of perfect-electric-conductor feeding the EMXT horn, and perfect matching boundaries around the antenna mimicking an infinite open space for the antenna radiation to propagate. The return loss obtained is less than -29.8 dB over the simulated frequency range from 90 to 170 GHz, showing a very good impedance matching between the antenna and the free space. Figure 5 depicts the far-field pattern of the EMXT horn antennas captured at its E-plane, with the azimuth angle sweeping from 0 to 360 degree. Center frequencies of two pass bands (114 GHz and 162 GHz) for the EMXT horn antenna are chosen to generate the plots. These simulated patterns clearly demonstrate directional beams from the EMXT antenna at its two working frequencies. Its directivity at the boresight is quite comparable with a copper horn antenna of exactly the same dimensions at its first working frequency 114 GHz, but ~ 9.4 dB higher at its second working frequency 162 GHz.

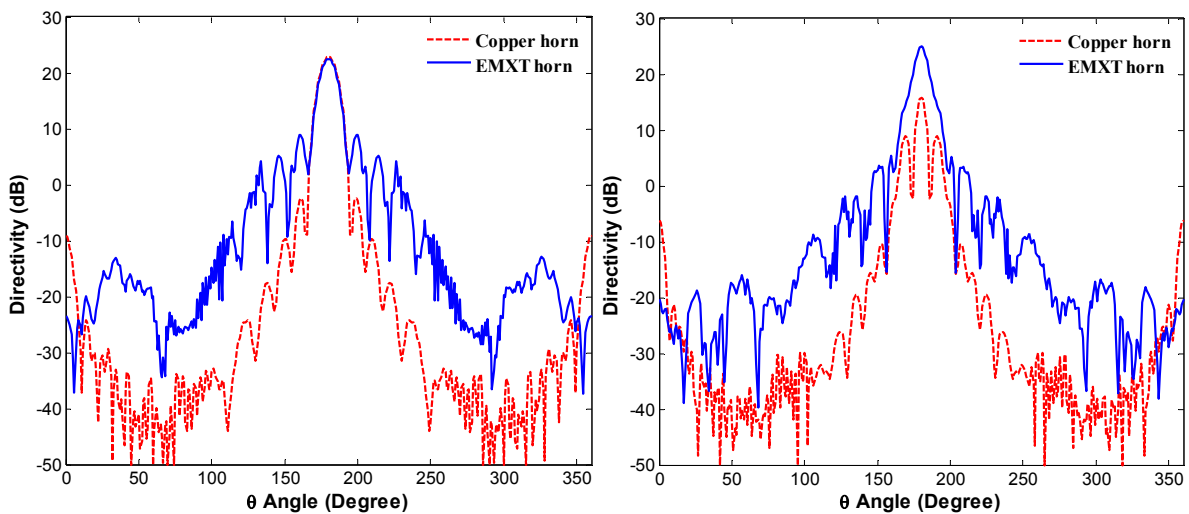


Figure 5. Radiation patterns of the EMXT and copper horn antenna at its E-plane with θ sweeping from 0 to 360 degrees, at 114 GHz (left) and 162 GHz (right).

Figure 6 shows two photo images of the fabricated EMXT horn antenna sample using the same rapid prototyping approach. From the side view, the flare-out of the horn shape is clearly observed, and the front view shows the horn tapered down to the straight waveguide feeding section. Experiments to characterize the radiation pattern of the fabricated EMXT horn antenna is currently undergoing.

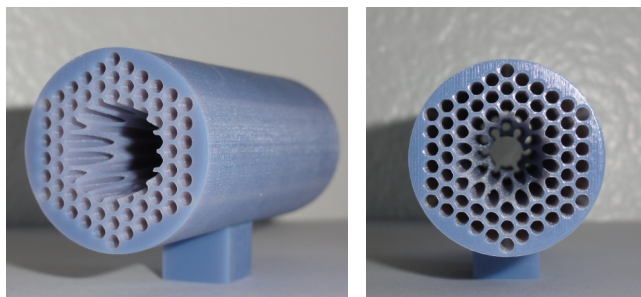


Figure 6. Photo images of the fabricated THz EMXT horn antenna.

2.5 Transition Structure to Planar Circuits

Given that the antenna element for free-space radiation coupling and the waveguide element for energy transport are realized, a transition structure from the waveguide section to a planar circuit would make the last element for a basic and self-contained THz transeiving system, if THz planar IC source and detector are integrated in the planar circuit. The transition structure could also be very useful in THz planar sample characterization, such as semiconducting devices and circuits, thin films, individual carbon nanotube (CNT) or CNT ensembles, etc. Based on the EMXT THz waveguide design aforementioned, a transition design to planar microstrip lines is also proposed. The figure below illustrates the transition in a back-to-back configuration.

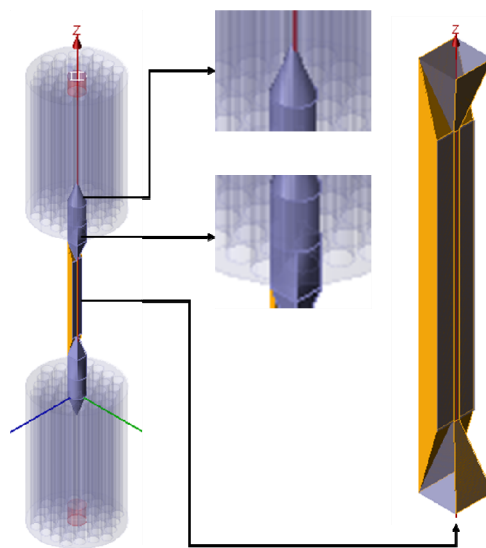


Figure 7. Schematic of the EMXT waveguide-to-microstrip line transition design. Three zoomed-in insets demonstrate different sections of the transition structure.

The transition consists of two EMXT waveguides on both ends feeding the transition structure and a planar circuit (simple microstrip line here) in the middle. The defect core radius of the EMXT waveguide is 2.1 mm and each

waveguide is 35 mm long. On each end, the transition structure is made of four sections. The first section is a tapered dielectric cone with circular cross-section, 5 mm height and 2.1 mm base radius as shown in the top middle inset of Figure 7. The cone is completely intruded into the EMXT waveguide by the distance of its height. This section, connecting the air region with the dielectric region by the taper, helps reduce reflection and couple the EMXT waveguide mode to the dielectric waveguide HE_{11} mode. The second section is simply a 5-mm long circular dielectric rod with the same 2.1 mm radius as shown in the bottom middle inset image. This section serves as a region to allow the dielectric waveguide mode to build up and stabilize. Also shown in the same inset, immediately following the second section is a 5-mm long dielectric section transforming the circular shaped cross-section to 4.2 mm x 4.2 mm square shape. The final transition section is a rectangular wedge with its cross-section tapered, over an axial distance of 5 mm, from the 4.2 mm x 4.2 mm square to a 0.4 mm x 0.127 mm rectangle, which exactly fits to the trace width and substrate thickness of the microstrip line. As illustrated in the right inset, two PEC ground flares (orange color) are placed on top and bottom surfaces of the dielectric wedge, which are connected to the center trace and the ground plane of the microstrip line respectively. These PEC flares form a wedged parallel plate waveguide and help compress the E-field spread across them. Figure 8 plots the simulated S_{21} (in dB) of the entire back-to-back transition with various losses included, which exhibits two pass bands corresponding to that of the EMXT waveguide feeds. Simulation results show good power transmission through this back-to-back transition structure, yielding a coupling loss of ~ 1 dB at each transition section after all the other losses are calibrated out.

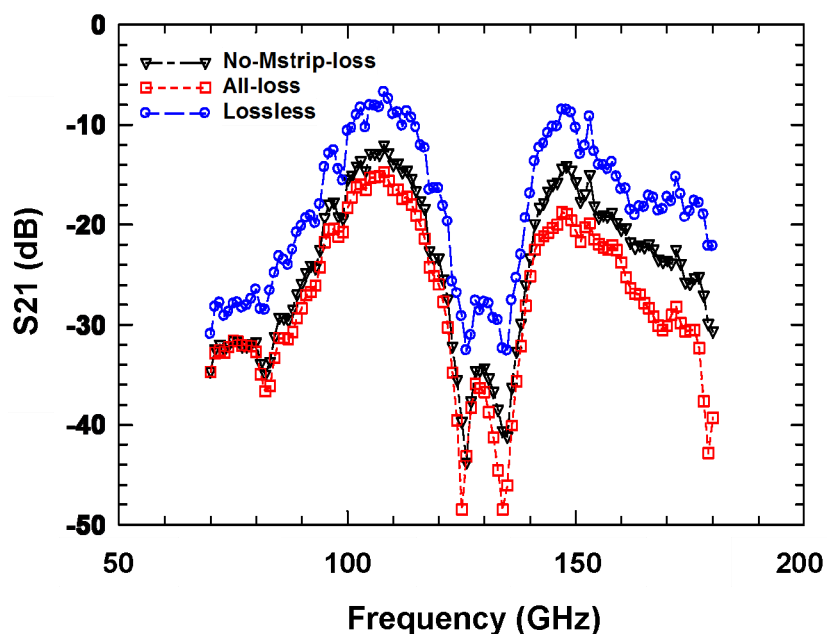


Figure 8. Simulated S_{21} (dB) of the entire EMXT waveguide-to-microstrip line-to-waveguide transition structure, including no-material-loss case, all-material-losses except the microstrip line section case, and all-material-losses case.

3. CONCLUSIONS

An efficient polymer-jetting rapid prototyping technique for THz fabrication has been developed which is particularly suitable for Fabrication of electromagnetic crystal (EMXT) based THz components. Various building block components of functionalities including filter/reflector, waveguide, antenna, and transition to planar circuits are proposed and simulated. Fabrications have been implemented for several of them, and the characterizations show very good agreement with the simulations. Potential integrated THz micro-systems, as well as THz integrated circuit (IC) characterization fixtures, could be constructed using these components. The layer-by-layer printing nature of the rapid prototyping technique may enable the integration and packaging of various THz components in a systematic manner.

REFERENCES

- [1] Siegel, P. H., "Terahertz technology," *IEEE Trans. Microwave Theory Tech.* 50 (3), 910-928 (2002).
- [2] Wu, Z., Kinast, J., Gehm, M. E. and Xin, H., "Rapid and inexpensive fabrication of terahertz electromagnetic bandgap structures," *Opt. Express* 16, 16442-16451 (2008).
- [3] Wu, Z., Ng, W. R., Gehm, M. E. and Xin, H., "All-dielectric low-loss terahertz waveguide fabricated by rapid prototyping," presented at 34th Int. Conf. Infrared, Millimeter and Terahertz Waves, Busan, Korea, Sep. 2009.
- [4] Joannopoulos, J. D., Johnson, S. G., Winn, J. N. and Meade, R. D., [*Photonic crystals: Molding the flow of the Light*], Princeton University Press, Princeton & Oxford, 156-189 (2008).
- [5] Atakaramians, S., Afshar, S. V., Fischer, B. M., Abbott, D. and Monro, T. M., "Porous fibers: a novel approach to low loss THz waveguides," *Opt. Express* 16, 8845-8854 (2008).